PHYSICAL REVIEW D **93,** 083012 (2016)

Massive photon and dark energy

Seyen Kouwn,[1,*] Phillial Oh,[2,†] and Chan-Gyung Park[3,‡]

[1]*Korea Astronomy and Space Science Institute, Daejeon 305-348, Republic of Korea*
[2]*Department of Physics, BK21 Physics Research Division, Institute of Basic Science, Sungkyunkwan University, Suwon 440-746, Korea*
[3]*Division of Science Education and Institute of Fusion Science, Chonbuk National University, Jeonju 561-756, Korea*

(Received 27 December 2015; published 29 April 2016)

We investigate the cosmology of massive electrodynamics and explore the possibility whether the massive photon could provide an explanation of dark energy. The action is given by the scalar-vector-tensor theory of gravity, which is obtained by nonminimal coupling of the massive Stueckelberg QED with gravity; its cosmological consequences are studied by paying particular attention to the role of photon mass. We find that the theory allows for cosmological evolution where the radiation- and matter-dominated epochs are followed by a long period of virtually constant dark energy that closely mimics a ΛCDM model. We also find that the main source of the current acceleration is provided by the nonvanishing photon mass governed by the relation $\Lambda \sim m^2$. A detailed numerical analysis shows that the nonvanishing photon mass on the order of $\sim 10^{-34}$ eV is consistent with current observations. This magnitude is far less than the most stringent limit on the photon mass available so far, which is on the order of $m \leq 10^{-27}$ eV.

DOI: 10.1103/PhysRevD.93.083012

I. INTRODUCTION

The intriguing discovery of the current accelerating Universe [1,2] has generated extensive investigations searching for a foundation that provides theoretical explanations. The simplest lambda cold dark matter (ΛCDM) model [3], with the cosmological constant Λ as dark energy, fits very well with observations and is regarded as the most accepted approach. To be consistent with current observations, the cosmological constant Λ has to be a very small number in value, $\sim 10^{-120}$ orders of magnitude smaller than the Planck scale $M_{\rm p}$; this extreme fine-tuning leads to the cosmological constant problem [4], which has spurred diverse other attempts in search of the origin of dark energy. One of the alternative methods is the quintessence model [5], in which the cosmological constant is a dynamically varying potential energy of a scalar field. Despite this model's simplicity and many attractive features, some problems remain. For example, it does not resolve the puzzle of cosmic coincidence, which seems to be a common feature of decaying cosmological constant (with a few exceptions) [6]. It also necessitates the introduction of a new scalar field, whereas the only experimentally verified available scalar field is the Higgs field.

One of the possible pathways to the cosmological constant problem may be to suppose that Λ is associated with another fundamental mass scale. One possible candidate is the UV cutoff of quantum field theory, based on the holographic principle [7] or the electroweak scale [8]; this can provide a natural explanation of the coincidence problem. Another possibility is that the smallness of Λ is related to yet another small number in nature; it would be conceivable, then, that there might exist some relation connecting them. It could come as a solution of the equations of motion, or might be a consequence of fundamental reason that is currently inaccessible. The first candidate that comes to mind is the mass of the photon, if it has a mass at all. In this paper, we investigate the cosmology of massive electrodynamics and explore the possibility whether a massive photon could provide an explanation of dark energy.

The photon mass is usually assumed to be exactly zero. This is based on the Maxwell equations which describe a massless photon. In addition, a photon mass term in quantum electrodynamics breaks gauge invariance and might spoil the renormalizability, which renders the theory quantum-mechanically inconsistent. However, the consideration of a nonvanishing photon mass [9] has a long history; theoretically, it is well known that Maxwell's theory with Abelian gauge symmetry can be extended to a gauge-invariant massive theory by means of the Stueckelberg mechanism [10].[1] This theory introduces a scalar field that compensates the gauge transformation of the vector field. Such a massive theory preserves the unitarity and renormalizability of the massless theory. Moreover, the possible conflict between the massive

*seyenkouwn@kasi.re.kr
†ploh@skku.edu
‡parkc@jbnu.ac.kr

[1]The photon can also become massive through spontaneous symmetry breaking via the Higgs mechanism [11], but this idea will not be pursued in this paper.

QED and standard model could be avoided [12]. In a particular gauge where the scalar field is set to zero, the massive theory reduces to the Proca theory, which describes electrodynamics of massive vector field [13]. The question of a photon mass in QED should then be tested experimentally. If there is any deviation from zero, it must be very small, because Maxwell theory has been verified to an extreme accuracy. On the other hand, the experimental constraints on the photon mass have considerably increased over the past several decades, putting upper bounds on its mass. So far, the most stringent upper limit is given by $m \leq 10^{-27}$ eV [14]. In all these studies, the photon is described by a massive Proca theory that does not include the Stueckelberg field.

There exist many attempts to link the cosmology of vector fields with the accelerating Universe [15,16], but direct cosmological consequences of the massive QED in relation to the dark energy have been considered only recently [17]. It was shown that the massive QED without the Stueckelberg field (but with the nonvanishing torsion components) has the potential to be a possible explanation of dark energy in terms of the photon mass, where the dark-energy density (cosmological constant), which is proportional to the photon mass squared, is allowed as a solution of equations of motion. In this work, we take the full massive QED including the scalar field and investigate the cosmology. The theory consists of a massive vector field and a Stuckelberg scalar field interacting with Einstein gravity. Also, for general purposes, we include nonminimal interaction terms in which the vector field interacts with the scalar curvature and the Ricci tensor.

The action contains a scalar field, which is necessary in order to endow the photon with mass while preserving the gauge invariance. Possible cosmological consequences of this Stueckelberg field were considered previously [18]. Its role in ordinary massive QED is to cancel the contribution of the unphysical pole of the vector propagator in the physical processes; it cannot appear as physical states (see [19] for a general introduction). This is evident because the field can be completely gauged away in the unitary gauge. However, such a decoupling of the Stueckelberg field does not operate when the gravitational interaction is included. The gravitational coupling can accommodate nonvanishing contributions of the Stueckelberg field. For example, in the massless limit of massive Proca theory, the longitudinal scalar mode remains coupled to gravitation, even though it is decoupled from the current [20]. The same reasoning will apply to the Stueckelberg scalar field with the covariant massive QED: it will also decouple from the current in the massless limit, but the gravitational coupling remains. Therefore, it cannot be neglected in cosmology; effectively, we are considering a nonminimally interacting scalar-vector-tensor (SVT) theory of gravity.

It is worth mentioning the gauge invariance of energy-momentum tensor of the covariant action. If we calculate the energy-momentum tensor of the covariant action of the Proca theory, for example, it will contain a gauge-dependent piece coming from the gauge-fixing term. However, this term becomes null if we apply the Lorentz gauge condition [see Eq. (2.6)], and the gauge invariance of the energy-momentum tensor is intact in quantum field theory. As far as cosmology is concerned, we might accept the effective action as a classical one and attempt to look for time-dependent behavior of the gauge field with only the temporal component being nonvanishing. This is necessary in order to respect the isotropy and homogeneity. In general, this will bring in a gauge dependence of the energy-momentum tensor [16]; however, this should not imply the inconsistency of the cosmological approach, but it could be taken as an indication of a characteristic of the gravitational interaction. It is interesting to note that in the pure electromagnetic case, the gauge-fixing term with only the temporal component of the gauge potential induces a vacuum energy or a cosmological constant whose value depends on the gauge-fixing parameter, but this is still harmless to the ordinary QED.

The purpose of this work is to study the cosmology of the SVT (or Einstein-Proca-Stueckelberg) theory of gravity, which is obtained by nonminimally coupling massive QED with gravity, and to compare the results with the observations, focusing especially on the photon mass. The SVT theory has several parameters with values that can be restricted by the observational constraints. A couple of the parameters are related to the cosmological solution that yields both decaying and growing modes; they can be fixed from the beginning by choosing the decaying mode conditions. These conditions allow cosmological evolution in which the radiation- and matter-dominated epochs are entailed by a long period of virtually constant dark energy, which mimics ΛCDM. The main source of dark energy is provided by the nonvanishing photon mass during this period. A detailed numerical analysis shows that the nonvanishing photon mass on the order of $\sim 10^{-34}$ eV is consistent with the current observations. This magnitude is far less than the most stringent limit on the photon mass available so far, which is on the order of $m \leq 10^{-27}$ eV [14].

The paper is organized as follows: In Sec. II, we construct Einstein-Proca-Stueckelberg theory of massive QED interacting with gravity and write equations of motion for Friedmann-Robertson-Walker cosmology. In Sec. III, we analyze the cosmological evolutions in the radiation-, matter-, and dark-energy-dominated epochs, respectively. In Sec. IV, observational constraints on our model parameters are presented. Section V includes conclusion and discussions.

II. MODEL

The action we consider is the gauge-fixed massive QED theory that is nonminimally interacting with the Einstein

gravity. Keeping terms only up to the second derivative of the fields brings us to the following:

$$S = \int d^4x\sqrt{-g}\Big[\frac{R}{2\kappa} - \frac{1}{4}F_{\mu\nu}F^{\mu\nu} - \frac{1}{2}m^2A_\mu A^\mu - \frac{1}{2\xi}(\nabla_\mu A^\mu)^2 - \frac{1}{2}\nabla_\mu\phi\nabla^\mu\phi - \frac{1}{2}\xi m^2\phi^2 + \omega A_\mu A^\mu R + \eta A^\mu A^\nu R_{\mu\nu} + \frac{\chi}{2}\phi^2 R\Big], \tag{2.1}$$

where $F_{\mu\nu} = \partial_\mu A_\nu - \partial_\nu A_\mu$, ξ is the gauge-fixing parameter, and ω, η, and χ are dimensionless parameters describing the nonminimal interactions.

A couple of comments are in order. The above action (2.1) in flat space reduces to the massive QED with the Stueckelberg scalar field in the covariant gauge. This is the most general second-derivative action that describes the nonminimal interaction of the Stueckelberg scalar and massive vector field with the Einstein gravity, and it belongs to the most simple scalar extension of the vector-metric theory of gravity [21].

The Einstein equations obtained from action (2.1) by varying with respect to the metric $g_{\mu\nu}$ can be written in the following way:

$$\frac{1}{\kappa}G_{\mu\nu} = T^{(\varphi)}_{\mu\nu} + m^2T^{(m^2)} + T^{(F_{\mu\nu})}_{\mu\nu} - \frac{1}{2\xi}T^{(\xi)}_{\mu\nu} + \omega T^{(\omega)}_{\mu\nu} + \eta T^{(\eta)}_{\mu\nu} + \frac{\chi}{2}T^{(\chi)}_{\mu\nu} + T^{(m,r)}_{\mu\nu}, \tag{2.2}$$

where $T^{(m,r)}_{\mu\nu}$ is the energy-momentum tensor corresponding to other fields (matter and radiation) and we have defined

$$T^{(\varphi)}_{\mu\nu} = \nabla_\mu\varphi\nabla_\nu\varphi + g_{\mu\nu}\left(-\frac{1}{2}\nabla_\alpha\varphi\nabla^\alpha\varphi - V(\varphi)\right), \tag{2.3}$$

$$T^{(m^2)}_{\mu\nu} = A_\mu A_\nu + g_{\mu\nu}\left(-\frac{1}{2}A_\alpha A^\alpha\right), \tag{2.4}$$

$$T^{(F_{\mu\nu})}_{\mu\nu} = F^\alpha_\mu F_{\nu\alpha} + g_{\mu\nu}\left(-\frac{1}{4}F_{\alpha\beta}F^{\alpha\beta}\right), \tag{2.5}$$

$$T^{(\xi)}_{\mu\nu} = 4A_{(\mu}\nabla_{\nu)}\nabla_\alpha A^\alpha - g_{\mu\nu}((\nabla_\alpha A^\alpha)^2 + 2A^\alpha\nabla_\alpha\nabla_\beta A^\beta), \tag{2.6}$$

$$T^{(\omega)}_{\mu\nu} = 2(\nabla_{(\mu}\nabla_{\nu)}A^2 - A_\mu A_\nu R - A_\alpha A^\alpha G_{\mu\nu} - g_{\mu\nu}\Box A^2), \tag{2.7}$$

$$T^{(\eta)}_{\mu\nu} = 2\nabla_\alpha\nabla_{(\mu}A_{\nu)}A^\alpha - 4A^\alpha R_{\alpha(\mu}A_{\nu)} - \Box A_\mu A_\nu + g_{\mu\nu}(A^\alpha A^\beta R_{\alpha\beta} - \nabla_\alpha\nabla_\beta A^\alpha A^\beta), \tag{2.8}$$

$$T^{(\chi)}_{\mu\nu} = 4\nabla_\mu\varphi\nabla_\nu\varphi - 2\varphi^2G_{\mu\nu} + 4\varphi\nabla_{(\mu}\nabla_{\nu)}\varphi - 2g_{\mu\nu}\Box\varphi^2, \tag{2.9}$$

where $\Box = \nabla_\mu\nabla^\mu$, $A^2 = A_\mu A^\mu$ and brackets in a pair of indices denoting symmetrization with respect to the corresponding indices. Apart from the Einstein equations, we can obtain a set of field equations for gauge A_μ and scalar fields φ by varying the action with respect to the vector and scalar field; this gives

$$\nabla_\nu F^{\mu\nu} + (m^2 - 2\omega R)A^\mu - 2\eta R^\mu_\nu A^\nu - \frac{1}{\xi}\nabla^\mu(\nabla_\alpha A^\alpha) = 0, \tag{2.10}$$

$$\Box\varphi - (\xi m^2 - \chi R)\varphi = 0. \tag{2.11}$$

In this work we shall study the isotropic and homogeneous flat cosmology. Thus, we consider the time-dependent vector field and scalar field, so that[2]

$$A_\mu = (f(t), 0, 0, 0), \qquad \varphi = \varphi(t), \tag{2.12}$$

and the space-time geometry is given by the flat Robertson-Walker metric,

$$ds^2 = -dt^2 + a^2(dx^2 + dy^2 + dz^2). \tag{2.13}$$

In this metric, the field equations for the vector and scalar can be rewritten as

$$\ddot{f} + 3H\dot{f} + 3\dot{H}f + \xi f[m^2 - 6(\eta + 4\omega)H^2 - 6(\eta + 2\omega)\dot{H}] = 0, \tag{2.14}$$

$$\ddot{\varphi} + 3H\dot{\varphi} - 6\chi(2H^2 + \dot{H})\varphi + m^2\xi\varphi = 0, \tag{2.15}$$

and the Einstein equations can be rewritten as follows:

$$\frac{3}{\kappa}H^2 = \rho^{(r)} + \rho^{(m)} + \rho^{(\mathrm{de})}, \tag{2.16}$$

$$-\frac{3}{\kappa}H^2 - \frac{2}{\kappa}\dot{H} = p^{(r)} + p^{(m)} + p^{(\mathrm{de})}, \tag{2.17}$$

where $H \equiv \dot{a}/a$ is the Hubble parameter and we added the standard radiation and matter energy densities. $\rho^{(\mathrm{de})}$ and $p^{(\mathrm{de})}$ are the energy density and pressure coming from the

[2]Note that the configuration (2.12) gives $F_{\mu\nu} = 0$, and does not contribute to the photon radiation energy. Also, we assume that the spatial average of the photon polarization vector $\vec{A}$ is zero, and that mixing between A_0 and $\vec{A}$ in Eqs. (2.6)–(2.8) can be neglected. The contribution of quadratic terms in $\vec{A}$ is treated separately and is included as the photon radiation energy in $T^{(r)}_{\mu\nu}$.

temporal component of the vector (tv) plus scalar (s) fields, and we interpret $\rho^{(\mathrm{de})}$ and $p^{(\mathrm{de})}$ as the dark-energy density and dark pressure. They are, respectively, given as follows:

$$\rho^{(\mathrm{de})} = \rho^{(\mathrm{tv})} + \rho^{(\mathrm{s})}, \qquad p^{(\mathrm{de})} = p^{(\mathrm{tv})} + p^{(\mathrm{s})}, \tag{2.18}$$

where

$$\rho^{(\mathrm{tv})} \equiv \frac{1}{\xi} f\ddot{f} - \frac{1}{2\xi}\dot{f}^2 + \frac{1}{2}m^2 f^2 + 6(\eta + 2\omega)Hf\dot{f} - \left(\frac{9}{2\xi} + 18\omega\right)H^2 f^2 - \left(6\eta - \frac{3}{\xi} + 12\omega\right)\dot{H}f^2, \tag{2.19}$$

$$\rho^{(\mathrm{s})} \equiv \frac{1}{2}\dot{\varphi}^2 + \frac{1}{2}m^2\xi\varphi^2 - 6\chi H\varphi\dot{\varphi} - 3\chi H^2\varphi^2, \tag{2.20}$$

$$p^{(\mathrm{tv})} \equiv \left(-2\eta + \frac{1}{\xi} - 4\omega\right)f\ddot{f} + \left(-2\eta + \frac{1}{2\xi} - 4\omega\right)\dot{f}^2 + \frac{1}{2}m^2 f^2 + \left(-8\eta + \frac{6}{\xi} - 8\omega\right)Hf\dot{f} + \left(-6\eta + \frac{9}{2\xi} - 6\omega\right)H^2 f^2 + \left(-4\eta + \frac{3}{\xi} - 4\omega\right)\dot{H}f^2, \tag{2.21}$$

$$p^{(\mathrm{s})} \equiv 2\chi\varphi\ddot{\varphi} + \left(\frac{1}{2} + 2\chi\right)\dot{\varphi}^2 - \frac{1}{2}m^2\xi\varphi^2 + 4\chi H\varphi\dot{\varphi} + 3\chi H^2\varphi^2 + 2\chi\dot{H}\varphi^2. \tag{2.22}$$

III. COSMOLOGICAL EVOLUTION

In this section we analyze the evolution equations by assuming that the universe in each stage is dominated by a barotropic perfect fluid with constant equation-of-state parameter $w_i = \rho_i/p_i (i = m, r)$ and later by $\rho^{(\mathrm{de})}$. Then, we check our results numerically.

A. Radiation-dominated epoch

In the radiation-dominated epoch, let us assume that the energy densities of the matter and the dark energy are negligible,

$$\rho^{(\mathrm{de})} \ll \rho^{(r)}, \qquad \rho^{(m)} \ll \rho^{(r)}, \tag{3.1}$$

so that the Hubble parameter H is given by

$$\frac{3}{\kappa}H^2 \simeq \frac{\rho_{r,0}}{a^4}, \tag{3.2}$$

where $\rho_{r,0}$ is the present value of the energy density of the radiation. In such a case, we obtain the field equations, which can be written as

$$a^2 f'' + 2af' + 6(\eta\xi - 1) \simeq 0, \tag{3.3}$$

$$a^2\varphi'' + 2a\varphi' \simeq 0, \tag{3.4}$$

where we neglect the mass of the photon with respect to the Hubble parameter and a prime indicates a derivative with respect to the scale factor. They have the following solutions:

$$f(a) = c_-^{(r)} a^{-\frac{1}{2} - \frac{\sqrt{25-24\eta\xi}}{2}} + c_+^{(r)} a^{-\frac{1}{2} + \frac{\sqrt{25-24\eta\xi}}{2}}, \tag{3.5}$$

$$\varphi(a) = \frac{d_-^{(r)}}{a} + d_+^{(r)}, \tag{3.6}$$

where $c_\pm^{(r)}$ and $d_\pm^{(r)}$ are integration constants. Here, we impose the conditions $c_-^{(r)} = 0$ and $d_-^{(r)} = 0$ in order to make the solutions nonsingular as $a \to 0$. Inserting the above solutions into (2.18) and assuming that $c_+^{(r)}$ and $d_+^{(r)}$ are being of order $\mathcal{O}(1)$, we obtain that the conditions (3.1) yields the restrictions

$$\eta\xi \lesssim 1, \qquad \chi \lesssim 0. \tag{3.7}$$

Concerning the evolutions of the temporal component of the gauge field and scalar field, according to (2.18), the dark energy and pressure are given by

$$\rho^{(\mathrm{de})} \simeq -\chi\frac{(d_+^{(r)})^2\kappa\rho_{r,0}}{a^4}, \qquad p^{(\mathrm{de})} \simeq -\frac{\chi}{3}\frac{(d_+^{(r)})^2\kappa\rho_{r,0}}{a^4}. \tag{3.8}$$

Here, we find that $\rho^{(\mathrm{tv})}$ and $p^{(\mathrm{tv})}$ are much smaller than those of the scalar field, and so we have neglected them. This is because the temporal component is proportional to the scale factor in such a way that its energy density and pressure scale with an exponent larger than -4. Thus, the leading behavior of the energy density and pressure comes from the scalar field. We can also calculate the equation-of-state parameter, which results in

$$w^{(\mathrm{de})} \equiv \frac{p^{(\mathrm{de})}}{\rho^{(\mathrm{de})}} \simeq \frac{1}{3}. \tag{3.9}$$

Here, we note that the dark energy scales as radiation. Therefore, during the radiation-dominated epoch the fraction of energy density, $\rho^{(r)}/\rho^{(\mathrm{de})}$, is a constant.

B. Matter-dominated epoch

In the matter-dominated epoch, we assume that the energy densities of the radiation and dark energy are negligible,

$$\rho^{(\mathrm{de})} \ll \rho^{(m)}, \qquad \rho^{(r)} \ll \rho^{(m)}, \tag{3.10}$$

so that the Hubble parameter H is given by

$$\frac{3}{\kappa}H^2 \simeq \frac{\rho_{m,0}}{a^3}, \tag{3.11}$$

where $\rho_{m,0}$ is the present value of the energy density of the matter. In such a case, the evolution equations can be written as

$$a^2 f'' + \frac{5}{2}af' + \left(3\eta\xi - 6\xi\omega - \frac{9}{2}\right)f \simeq 0, \tag{3.12}$$

$$a^2\varphi''(a) + \frac{5}{2}a\varphi'(a) \simeq 0, \tag{3.13}$$

and they have the following solutions:

$$f(a) \simeq c_-^{(m)}a^{-\frac{\beta}{4}-\frac{3}{4}} + c_+^{(m)}a^{\frac{\beta}{4}-\frac{3}{4}}, \tag{3.14}$$

$$\varphi(a) \simeq \frac{d_-^{(m)}}{a^{3/2}} + d_+^{(m)}. \tag{3.15}$$

Here $c_\pm^{(m)}$ and $d_\pm^{(m)}$ are integration constants from the viewpoints of the differential equations, but they should satisfy the continuity of the evolution coming from the radiation-dominated epoch. β is defined by

$$\beta \equiv \sqrt{-48\eta\xi + 96\xi\omega + 81}. \tag{3.16}$$

We see that the solutions of the temporal component of the gauge field have two different types of evolution depending on whether β is real or imaginary. So, if the term $-48\eta\xi + 96\xi\omega + 81$ inside the square root is a positive real number, the corresponding solution of the gauge field will evolve as a power law given by growing ($\beta > 3$) or decaying ($\beta < 3$) modes. On the other hand, if the term inside the square root is negative, the gauge field will oscillate with an amplitude proportional to $a^{-3/4}$,

$$f(a) \simeq \frac{(c_-^{(m)} + c_+^{(m)})\cos\left(\frac{\mathrm{Im}(\beta)}{4}\ln a\right)}{a^{3/4}}, \tag{3.17}$$

where $c_1 = c_2$ for real values of the $f(a)$. Another possibility remaining is when we have $\beta = 3$. Then, the corresponding solution will converge to a constant during the matter-domination epoch,

$$f(a) \simeq \frac{c_-^{(m)}}{a^{3/2}} + c_+^{(m)}. \tag{3.18}$$

Concerning the evolutions of temporal component of the massive photon field and scalar field, according to (2.18), the dark energy and pressure are given by[3]

$$\rho^{(\mathrm{de})} \simeq \frac{m^2\xi}{2}\left(d_-^{(m)} + \frac{d_+^{(m)}}{a^{3/2}}\right)^2, \tag{3.19}$$

$$p^{(\mathrm{de})} \simeq -\frac{m^2\xi}{2}\left(d_-^{(m)} + \frac{d_+^{(m)}}{a^{3/2}}\right)^2, \tag{3.20}$$

and we can also calculate the equation of state parameter as

$$w^{(\mathrm{de})} \equiv \frac{p^{(\mathrm{de})}}{\rho^{(\mathrm{de})}} \simeq -1. \tag{3.21}$$

Therefore, we note that as the universe expands, we have $\rho^{(\mathrm{de})} \to (d_-^{(m)})^2 m^2\xi/2$ and $p^{(\mathrm{de})} \to -(d_-^{(m)})^2 m^2\xi/2$ with $w^{(\mathrm{de})} \to -1$, so that the scalar component of the massive photon field furnishes the main source of dark energy in this epoch.

C. Dark-energy-dominated epoch

In this section we shall study the case in which the late-time Universe becomes dominated by dark energy,

$$\rho^{(r)} \ll \rho^{(\mathrm{de})}, \qquad \rho^{(m)} \ll \rho^{(\mathrm{de})}, \tag{3.22}$$

so that the Friedmann equations are given by

$$\frac{3}{\kappa}H^2 \simeq \rho^{(\mathrm{de})}, \tag{3.23}$$

$$-\frac{3}{\kappa}H^2 - \frac{2}{\kappa}\dot{H} \simeq p^{(\mathrm{de})}. \tag{3.24}$$

For the subsequent analysis, it will be convenient to introduce the following ansatz for the dark-energy density[4]:

$$\rho^{(\mathrm{de})} \simeq \frac{\rho_*^{(\mathrm{de})}}{a^n}, \tag{3.25}$$

where n is a constant number that will be determined by the dynamical equations. The Hubble parameter H is given by

[3]We consider only decaying modes for the temporal vector component evolution. Their contributions to energy density and pressure can then be neglected again because they remain substantially smaller than the scalar contributions during the radiation-dominated epoch, which is followed by the decaying-mode contribution of Eq. (3.14).

[4]It turns out that the evolution equations (3.23) and (3.24) admit a series solution in terms of inverse power of the scale factor a. Since the higher-order terms decay rapidly with the expansion of the Universe, we only consider the leading behavior, which is sufficient for our purpose and which is supported by numerical analysis.

$$\frac{3}{\kappa}H^2 \simeq \frac{\rho_*^{(\mathrm{de})}}{a^n}, \tag{3.26}$$

where $\rho_*^{(\mathrm{de})}/a_*^n$ is the dark-energy density when its dominance (3.22) takes place, i.e., $a = a_*$. In such a case, the corresponding field equations are given by

$$a^2 f'' + \left(4 - \frac{n}{2}\right) a f' + W^{(f)} f \simeq 0, \tag{3.27}$$

$$a^2 \varphi'' + \left(4 - \frac{n}{2}\right) a \varphi' + W^{(\varphi)} \varphi \simeq 0, \tag{3.28}$$

with $W^{(f)}$ and $W^{(\varphi)}$ defined by

$$W^{(f)} \equiv \frac{3m^2\xi}{\kappa\rho_*^{(\mathrm{de})}} a^n - 6\xi(\eta + 4\omega) + n\left(3\eta\xi + 6\omega\xi - \frac{3}{2}\right), \tag{3.29}$$

$$W^{(\varphi)} \equiv \frac{3m^2\xi}{\kappa\rho_*^{(\mathrm{de})}} a^n + 3(n-4)\chi. \tag{3.30}$$

For the nonzero positive values, $n > 0$, the values of $W^{(f)}$ and $W^{(\varphi)}$ are dominated by the a^n term, so we can use the approximation with $W \equiv \frac{3m^2\xi}{\kappa\rho_*^{(\mathrm{de})}}$,

$$W^{(f)} \simeq W a^n, \qquad W^{(\varphi)} \simeq W a^n. \tag{3.31}$$

The corresponding solutions are given by

$$f \simeq \frac{1}{a^{3/2}}\left[c_-^{(v)} \cos\left(\frac{2\sqrt{W}}{n} a^{n/2} - \frac{3\pi}{2n}\right) + c_+^{(v)} \sin\left(\frac{2\sqrt{W}}{n} a^{n/2} + \frac{3\pi}{2n}\right)\right], \tag{3.32}$$

$$\varphi \simeq \frac{1}{a^{3/2}}\left[d_-^{(v)} \cos\left(\frac{2\sqrt{W}}{n} a^{n/2} - \frac{3\pi}{2n}\right) + d_+^{(v)} \sin\left(\frac{2\sqrt{W}}{n} a^{n/2} + \frac{3\pi}{2n}\right)\right], \tag{3.33}$$

where $c_\pm^{(v)}$ and $d_\pm^{(v)}$ are integration constants. Here, we note that when we insert the above solutions into (2.18), Eq. (3.22) forces $n = 3$, and thus the corresponding energy density and pressure of the massive vector field are given by

$$\rho^{(\mathrm{de})} \simeq \frac{m^2\xi/2}{a^3}\left[(d_-^{(v)})^2 + (d_+^{(v)})^2 - \frac{(c_-^{(v)})^2 + (c_+^{(v)})^2}{\xi}\right], \tag{3.34}$$

$$p^{(\mathrm{de})} \simeq \frac{m^2\xi/2}{a^3}\left[p_+ \sin\left(\frac{4}{3}a^{3/2}\sqrt{W}\right) + p_- \cos\left(\frac{4}{3}a^{3/2}\sqrt{W}\right)\right], \tag{3.35}$$

where p_+ and p_- are the amplitudes given by

$$p_+ \equiv 2c_-^{(v)}c_+^{(v)}\left(4\eta + 8\omega - \frac{1}{\xi}\right) - 2d_-^{(v)}d_+^{(v)}, \tag{3.36}$$

$$p_- \equiv ((c_-^{(v)})^2 - (c_+^{(v)})^2)\left(-4\eta - 8\omega + \frac{1}{\xi}\right) + (d_-^{(v)})^2 - (d_+^{(v)})^2. \tag{3.37}$$

Note that if (3.34) is exactly correct then the corresponding pressure should be zero. But it shows only the leading behavior in the expansion. If, for example, we calculate the next order, $\rho^{(\mathrm{de})}$ will be augmented by an oscillating term whose magnitude decays as power of $\sim 1/a^{9/2}$, as was

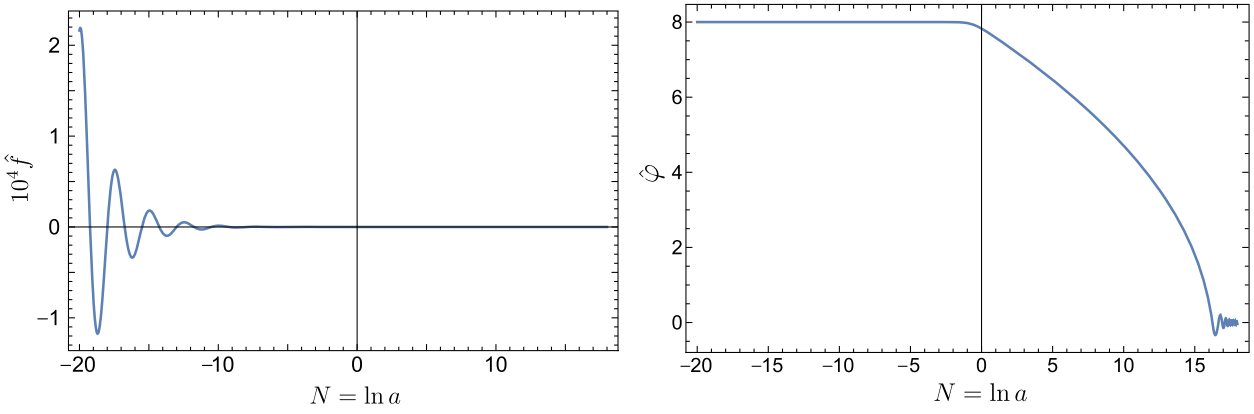

FIG. 1. Evolution of $\hat{f}$ (left) and $\hat{\varphi}$ (right) as a function of logarithmic scale factor $N = \ln a(t)$. In both panels, we have used $\hat{\eta} = 0.9$, $\hat{\omega} = -0.35$, $\chi = 10^{-7}$, and $\hat{m} = 10^{-3}$. We have also set the initial values $\hat{\varphi}_i = 8$ and $\hat{f}_i \simeq a_i^{(1+\sqrt{25-24\hat{\eta}})/2} \simeq 2 \times 10^{-4}$ at the initial epoch $\ln a_i = -20$.

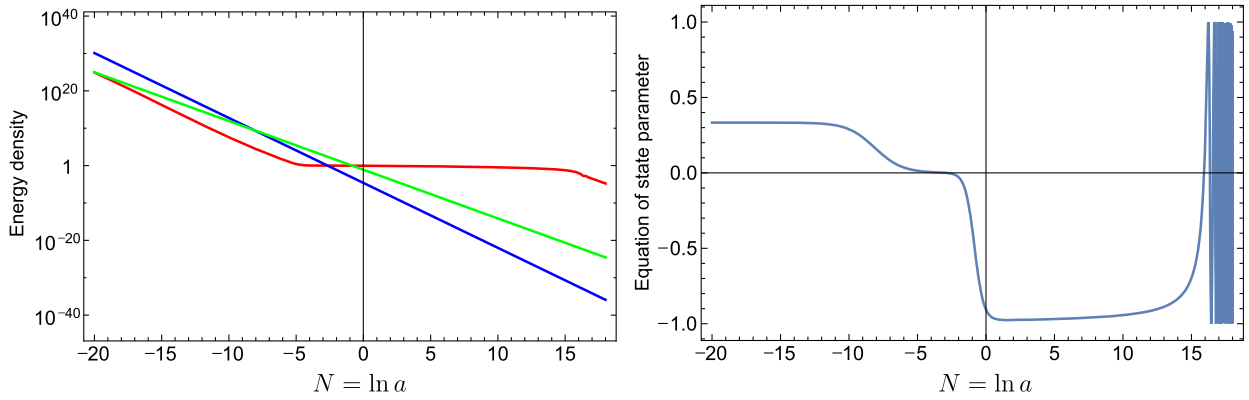

FIG. 2. (Left) Evolution of energy density of the vector field (red), radiation (blue), and matter (green curve). (Right) Evolution of the equation-of-state parameter. The same model parameters have been used as in Fig. 1.

mentioned before. Then, the equation-of-state parameter for the dark energy is given by

$$\omega^{(\mathrm{de})} = \frac{p^{(\mathrm{de})}}{\rho^{\mathrm{de}}} \simeq \frac{p_+ \sin\left(\frac{4\sqrt{W}}{3} a^{3/2}\right) + p_- \cos\left(\frac{4\sqrt{W}}{3} a^{3/2}\right)}{(d_-^{(v)})^2 + (d_+^{(v)})^2 - \frac{(c_-^{(v)})^2 + (c_+^{(v)})^2}{\xi}}. \tag{3.38}$$

We note that the equation-of-state parameter has oscillation terms which gives zero average value. Thus, the corresponding energy density should be proportional to $1/a^3$, which is consistent with energy density equation (3.34). In Fig. 1, we plot behaviors of f and φ based on numerical solutions to confirm our analytically approximated solution. Figure 2 shows that the dark-energy density decreases as a^{-4} during the early radiation-dominated epoch, remains almost constant during the matter-dominated epoch, and then it decreases again as a^{-3} in the dark-energy-dominated era.

IV. OBSERVATIONAL CONSTRAINTS

In this section we will confront our model with the latest cosmological data and study whether it can be distinguished from the ΛCDM model. For this purpose, we use recent observational data such as type Ia supernovae (SN), baryon acoustic oscillation (BAO) based on large-scale structure of galaxies, cosmic microwave background (CMB) radiation, and Hubble parameters $[H(z)]$. For numerical analysis, it is convenient to rewrite Eqs. (2.14)–(2.16) in terms of $N \equiv \ln a$ as follows:

$$\begin{aligned}\hat{H}^2 = {} & \frac{1}{6}\hat{m}^2\hat{\varphi}^2 - \frac{1}{6}\hat{m}^2\hat{f}^2 \\ & + \frac{\hat{H}^2}{3}\left[\hat{f}^2\left(6\hat{\eta} - \frac{9}{2} + 6\hat{\omega}\right) - 3\chi\hat{\varphi}^2 + \frac{1}{2}(\hat{\varphi}'^2 - \hat{f}'^2) + \hat{f}\hat{f}'(6\hat{\eta} - 3 + 12\hat{\omega}) - 6\chi\hat{\varphi}\hat{\varphi}'\right] \\ & + \Omega_r h^2 e^{-4N} + \Omega_m h^2 e^{-3N},\end{aligned} \tag{4.1}$$

where a prime indicates a derivative with respect to N, and

$$\begin{aligned}\hat{H}^2\hat{f}'' + (\hat{H}\hat{H}' + 3\hat{H}^2)\hat{f}' + [\hat{m}^2 - 3\hat{H}\hat{H}'(-1 + 2\hat{\eta} + 4\hat{\omega}) - 6\hat{H}^2(\hat{\eta} + 4\hat{\omega})]\hat{f} = 0, \\ \hat{H}^2\hat{\varphi}'' + (\hat{H}\hat{H}' + 3\hat{H}^2)\hat{\varphi}' + (\hat{m}^2 - 6\chi\hat{H}\hat{H}' - 12\chi\hat{H}^2)\hat{\varphi} = 0,\end{aligned} \tag{4.2}$$

where we have eliminated the second-order derivative in (4.1) by using the field equations, and have introduced dimensionless quantities,

$$\begin{aligned}&\hat{H}^2 \equiv \frac{H^2h^2}{H_0^2}, \qquad \Omega_r \equiv \frac{\kappa\rho_{r,0}}{3H_0^2}, \qquad \Omega_m \equiv \frac{\kappa\rho_{m,0}}{3H_0^2}, \qquad \hat{m}^2 \equiv \frac{m^2\xi h^2}{H_0^2}, \\ &\hat{f} \equiv \frac{\kappa f}{\xi}, \qquad \hat{\varphi} \equiv \kappa\varphi, \qquad \hat{\eta} = \eta\xi, \qquad \hat{\omega} = \omega\xi.\end{aligned} \tag{4.3}$$

Here, H_0 is the present value of the Hubble parameter, usually expressed as $H_0 = 100h\ \mathrm{km\,s^{-1}\,Mpc^{-1}}$, and Ω_r and Ω_m are the current density parameters of radiation and matter, respectively. The radiation density includes the contribution of relativistic neutrinos as well as that of photons, with the collective density parameter

$$\Omega_r h^2 = \Omega_\gamma h^2 (1 + 0.2271 N_{\mathrm{eff}}), \tag{4.4}$$

where $N_{\mathrm{eff}} = 3.04$ is the effective number of neutrino species, and Ω_γ is the photon density parameter with values of $\Omega_r = 2.470\,37 \times 10^{-5} h^{-2}$ for the present CMB temperature $T_0 = 2.725$ K (WMAP9) and $\Omega_r = 2.472\,18 \times 10^{-5} h^{-2}$ for $T_0 = 2.7255$ K (PLANCK). Notice that, in this analysis, we shall choose the decaying mode for the vector field $\hat{f}$ during the matter era, which satisfies a condition $\sqrt{-48\hat{\eta} + 96\hat{\omega} + 81} < 3$ in (3.16). In such a case, the contribution of the temporal component is negligible relative to the scalar field, and the decaying-mode condition gives almost the same probability in the parameter constraints for $\hat{\eta}$ and $\hat{\omega}$. Thus, we choose $\hat{\eta} = 0.9$ and $\hat{\omega} = -0.35$ as fixed values during our analysis.[5] Therefore, the background dynamics is completely determined by a set of parameters $(\hat{m}, \chi, \hat{\varphi}_i, \Omega_m)$. However, to confront our model with real observational data, we need an additional parameter of baryon density (Ω_b); lastly, our model also has five free parameters $\boldsymbol{\theta} = (\log_{10}\hat{m}, -\log_{10}(-\chi), \log_{10}\hat{\varphi}_i, \Omega_b h^2, \Omega_m h^2)$. It should be emphasized that the Hubble constant (H_0) is no longer a free parameter because it is derived from the integration of field equations for a given set of parameters chosen. The free parameters are taken in the following priors: $\log_{10}\hat{m} = [-3, 3]$, $-\log_{10}(-\chi) = [1, 7]$, $\log_{10}\hat{\varphi}_i = [-3, 3]$, $\Omega_b h^2 = [0.015, 0.030]$, and $\Omega_m h^2 = [0.11, 0.15]$. In addition, as mentioned above, we fixed the parameters as $\hat{\eta} = 0.9$ and $\hat{\omega} = -0.35$ for the analysis. To obtain the likelihood distributions for model parameters, we use the Markov chain Monte Carlo (MCMC) method based on the Metropolis-Hastings algorithm to randomly explore the parameter space that is favored by observational data [24]. The method needs to make decisions for accepting or rejecting a randomly chosen chain element via the probability function $P(\boldsymbol{\theta}|\mathbf{D}) \propto \exp(-\chi^2/2)$, where $\mathbf{D}$ denotes the data, and $\chi^2 = \chi^2_{H(z)} + \chi^2_{\mathrm{SN}} + \chi^2_{\mathrm{BAO}} + \chi^2_{\mathrm{CMB}}$ is the sum of individual chi-squares for $H(z)$, SN, BAO, and CMB data (defined below). During the MCMC analysis, we use a simple diagnostic to test the convergence of MCMC chain: the means estimated from the first (after the burn-in process) and the last 10% of the chain are approximately equal to each other if the chain has converged (see Appendix B of Ref. [25]).

[5]There are strong constraints from local gravity experiments which, among others, imply a small value for the ω parameter. In our case, $f^2\omega \ll 1$ and the parametrized Post-Newtonian γ parameter [22] is very close to unity, which does not cause enough change of the gravitational constant to be incompatible with the observation, that is, $|\gamma - 1| < 2 \times 10^{-5}$ [23].

A. Hubble parameters

In our analysis, we use 29 observational data points of Hubble parameters over a redshift range of $0.07 \leq z \leq 2.34$, which include 23 data points obtained from the differential age approach [26] and 6 derived from the BAO measurements [27]. The chi-square is defined as

$$\chi^2_{H(z)} = \sum_{i=1}^{29} \frac{[H_{\mathrm{th}}(z_i) - H_{\mathrm{obs}}(z_i)]^2}{\sigma_H^2(z_i)}, \tag{4.5}$$

where $H_{\mathrm{th}}(z_i)$ and $H_{\mathrm{obs}}(z_i)$ are theory-predicted and observed values of the Hubble parameter at redshift z_i, respectively, and σ_H denotes the measurement error of the observed data point.

B. Type Ia supernovae

The type Ia supernovae provide tight constraints on the energy content of the late-time Universe. We use the Union 2.1 compilation [28] that includes 580 SN over a redshift range $0.015 \leq z \leq 1.414$. In our analysis, we apply the chi-square that has been marginalized over the zero-point uncertainty due to absolute magnitude and Hubble constant [29],

$$\chi^2_{\mathrm{SN}} = c_1 - c_2^2/c_3, \tag{4.6}$$

where

$$c_1 = \sum_{i=1}^{580} \left[\frac{\mu_{\mathrm{th}}(z_i) - \mu_{\mathrm{obs}}(z_i)}{\sigma_i}\right]^2,$$
$$c_2 = \sum_{i=1}^{580} \frac{\mu(z_i)_{\mathrm{th}} - \mu_{\mathrm{obs}}(z_i)}{\sigma_i^2}, \qquad c_3 = \sum_{i=1}^{580} \frac{1}{\sigma_i^2}, \tag{4.7}$$

where $\mu_{\mathrm{obs}}(z_i)$ and σ_i denote the observed distance modulus and its measurement error of SN at redshift z_i. The theoretical distance modulus μ_{th} is defined as

$$\mu_{\mathrm{th}}(z) = 5\log[(1+z)r(z)], \tag{4.8}$$

where $r(z)$ is the comoving distance at redshift z,

$$r(z) = \frac{c}{H_0\sqrt{\Omega_k}} \sin\left[\sqrt{\Omega_k}\int_0^z \frac{H_0}{H(z')}\,dz'\right], \tag{4.9}$$

with c the speed of light and Ω_k the current density parameter of spatial curvature ($\Omega_k = 0$ in our analysis).

C. Baryon acoustic oscillations

We use an effective distance measure related to the BAO scale [30],

$$D_V(z) \equiv \left[r^2(z) \frac{cz}{H(z)} \right]^{\frac{1}{3}}, \tag{4.10}$$

and a fitting formula for the redshift of drag epoch (z_d) [31],

$$z_d = \frac{1291(\Omega_m h^2)^{0.251}}{1+0.659(\Omega_m h^2)^{0.828}} [1 + b_1 (\Omega_b h^2)^{b_2}], \tag{4.11}$$

where

$$b_1 = 0.313(\Omega_m h^2)^{-0.419}[1+0.607(\Omega_m h^2)^{0.674}],$$
$$b_2 = 0.238(\Omega_m h^2)^{0.223}. \tag{4.12}$$

As the BAO parameter, we use six numbers of $r_s(z_d)/D_V(z)$ extracted from the Six-Degree-Field Galaxy Survey [32], the Sloan Digital Sky Survey Data Release 7 and 9 [33], and the WiggleZ Dark Energy Survey [34], where $r_s(z)$ is the comoving sound horizon size. These BAO data points were used in the WMAP nine-year analysis [35]. Since the sound speed of baryon fluid coupled with photons (γ) is given as

$$c_s^2 = \frac{\dot{p}}{\dot{\rho}} = \frac{\frac{1}{3}\dot{\rho}_\gamma}{\dot{\rho}_\gamma + \dot{\rho}_b} = \frac{1}{3[1+(3\Omega_b/4\Omega_\gamma)a]}, \tag{4.13}$$

the comoving sound horizon size before the last scattering becomes

$$r_s(z) = \int_0^t c_s dt'/a = \frac{1}{\sqrt{3}} \int_0^{1/(1+z)} \frac{da}{a^2 H(a)[1+(3\Omega_b/4\Omega_\gamma)a]^{\frac{1}{2}}}. \tag{4.14}$$

The BAO measurements provide the following distance ratios [35]:

$$\langle r_s(z_d)/D_V(0.1)\rangle = 0.336,$$
$$\langle D_V(0.35)/r_s(z_d)\rangle = 8.88, \tag{4.15}$$

$$\langle D_V(0.57)/r_s(z_d)\rangle = 13.67,$$
$$\langle r_s(z_d)/D_V(0.44)\rangle = 0.0916, \tag{4.16}$$

$$\langle r_s(z_d)/D_V(0.60)\rangle = 0.0726,$$
$$\langle r_s(z_d)/D_V(0.73)\rangle = 0.0592. \tag{4.17}$$

The inverse of the covariance matrix between measurement errors is

$$\mathbf{C}_{\rm BAO}^{-1} = \begin{pmatrix} 4444.4 & 0 & 0 & 0 & 0 & 0 \\ 0 & 34.602 & 0 & 0 & 0 & 0 \\ 0 & 0 & 20.661157 & 0 & 0 & 0 \\ 0 & 0 & 0 & 24532.1 & -25137.7 & 12099.1 \\ 0 & 0 & 0 & -25137.7 & 134598.4 & -64783.9 \\ 0 & 0 & 0 & 12099.1 & -64783.9 & 128837.6 \end{pmatrix}. \tag{4.18}$$

The chi-square is given as

$$\chi^2_{\rm BAO} = \mathbf{X}^T \mathbf{C}^{-1}_{\rm BAO} \mathbf{X}, \tag{4.19}$$

where

$$\mathbf{X} = \begin{pmatrix} r_s(z_d)/D_V(0.1) - 0.336 \\ D_V(0.35)/r_s(z_d) - 8.88 \\ D_V(0.57)/r_s(z_d) - 13.67 \\ r_s(z_d)/D_V(0.44) - 0.0916 \\ r_s(z_d)/D_V(0.60) - 0.0726 \\ r_s(z_d)/D_V(0.73) - 0.0592 \end{pmatrix}. \tag{4.20}$$

D. Cosmic microwave background radiation

As the CMB data, we use the CMB distance priors based on WMAP nine-year data [35] and Planck data [36] for testing our model. The first distance measure is the acoustic scale l_A defined as

$$l_A = \pi \frac{r(z_*)}{r_s(z_*)}. \tag{4.21}$$

The decoupling epoch z_* can be calculated from the fitting function [37],

$$z_* = 1048[1+0.00124(\Omega_b h^2)^{-0.738}][1+g_1(\Omega_m h^2)^{g_2}], \tag{4.22}$$

where

$$g_1 = \frac{0.0783(\Omega_b h^2)^{-0.238}}{1+39.5(\Omega_b h^2)^{0.763}}, \qquad g_2 = \frac{0.560}{1+21.1(\Omega_b h^2)^{1.81}}. \tag{4.23}$$

The second distance measure is the shift parameter R which is given by

$$R(z_*) = \frac{\sqrt{\Omega_m H_0^2}}{c} r(z_*). \tag{4.24}$$

Recently, Shafer and Huterer [38] derived distance priors from the WMAP and Planck data and provided mean values and covariance matrix of the parameter combination (l_a, R, z_*) as an efficient summary of CMB information on dark energy. Hereafter, we use these data sets to constrain our model parameters.

1. WMAP nine-year data

According to WMAP nine-year observations (WMAP9) [35], the mean values for the three parameters (l_A, R, z_*) are given as [38]

$$\langle l_A(z_*)\rangle = 301.98, \qquad \langle R(z_*)\rangle = 1.7302, \qquad \langle z_*\rangle = 1089.09, \tag{4.25}$$

with their inverse covariance matrix

$$\mathbf{C}^{-1}_{\mathrm{WMAP9}} = \begin{pmatrix} 3.13365 & 15.1332 & -1.43915 \\ 15.1332 & 13343.7 & -223.16 \\ -1.43915 & -223.16 & 5.44598 \end{pmatrix}. \tag{4.26}$$

The chi-square is given as

$$\chi^2_{\mathrm{WMAP9}} = \mathbf{X}^T \mathbf{C}^{-1}_{\mathrm{WMAP9}} \mathbf{X}, \tag{4.27}$$

where

$$\mathbf{X} = \begin{pmatrix} l_A(z_*) - 301.98 \\ R(z_*) - 1.7302 \\ z_* - 1089.09 \end{pmatrix}. \tag{4.28}$$

2. Planck data

According to Planck observations (PLANCK) [36], the mean values for the three parameters (l_A, R, z_*) are given as [38]

$$\langle l_A(z_*)\rangle = 301.65, \qquad \langle R(z_*)\rangle = 1.7499, \qquad \langle z_*\rangle = 1090.41. \tag{4.29}$$

Their inverse covariance matrix is

$$\mathbf{C}^{-1}_{\mathrm{Planck}} = \begin{pmatrix} 42.7223 & -419.678 & -0.765895 \\ -419.678 & 57394.2 & -762.352 \\ -0.765895 & -762.352 & 14.6999 \end{pmatrix}. \tag{4.30}$$

The chi-square is given as

$$\chi^2_{\mathrm{Planck}} = \mathbf{X}^T \mathbf{C}^{-1}_{\mathrm{Planck}} \mathbf{X}, \tag{4.31}$$

where

$$\mathbf{X} = \begin{pmatrix} l_A(z_*) - 301.65 \\ R(z_*) - 1.7499 \\ z_* - 1090.41 \end{pmatrix}. \tag{4.32}$$

E. Results

We explore the allowed ranges of our dark-energy model parameters using the recent observational data by applying the MCMC parameter estimation method. In the

TABLE I. Summary of parameter constraints.

	Massive photon model		ΛCDM model	
	$H(z)$ + SN + BAO +WMAP9	$H(z)$ + SN + BAO +PLANCK	$H(z)$ + SN + BAO +WMAP9	$H(z)$ + SN + BAO +PLANCK
H_0	$69.57^{+0.84}_{-0.85}$	$69.21^{+0.71}_{-0.66}$	$69.57^{+0.83}_{-0.80}$	$69.32^{+0.67}_{-0.69}$
$\log_{10}\hat{m}$	$-0.8089^{+0.3718}_{-0.5758}$	$-0.8400^{+0.3200}_{-0.5393}$	...	...
$-\log_{10}(-\chi)$	$>4.1(2\sigma)$	$>4.3(2\sigma)$	...	...
$\Omega_m h^2$	$0.1409^{+0.0024}_{-0.0024}$	$0.1448^{+0.0016}_{-0.0014}$	$0.1410^{+0.0022}_{-0.0024}$	$0.1446^{+0.0014}_{-0.0015}$
$\Omega_b h^2$	$0.0240^{+0.0005}_{-0.0004}$	$0.0239^{+0.0003}_{-0.0003}$	$0.0239^{+0.0004}_{-0.0004}$	$0.0239^{+0.0003}_{-0.0003}$
$\log_{10}\hat{\varphi}_i$	$0.9586^{+0.5751}_{-0.3620}$	$0.9898^{+0.5364}_{-0.3161}$	...	...
$\Omega_\Lambda h^2$	...	...	$0.3433^{+0.0120}_{-0.0118}$	$0.3355^{+0.0105}_{-0.0105}$
χ^2_{min}	588.391	590.804	588.366	590.724
χ^2_ν	0.961 42	0.965 36	0.958 25	0.962 09

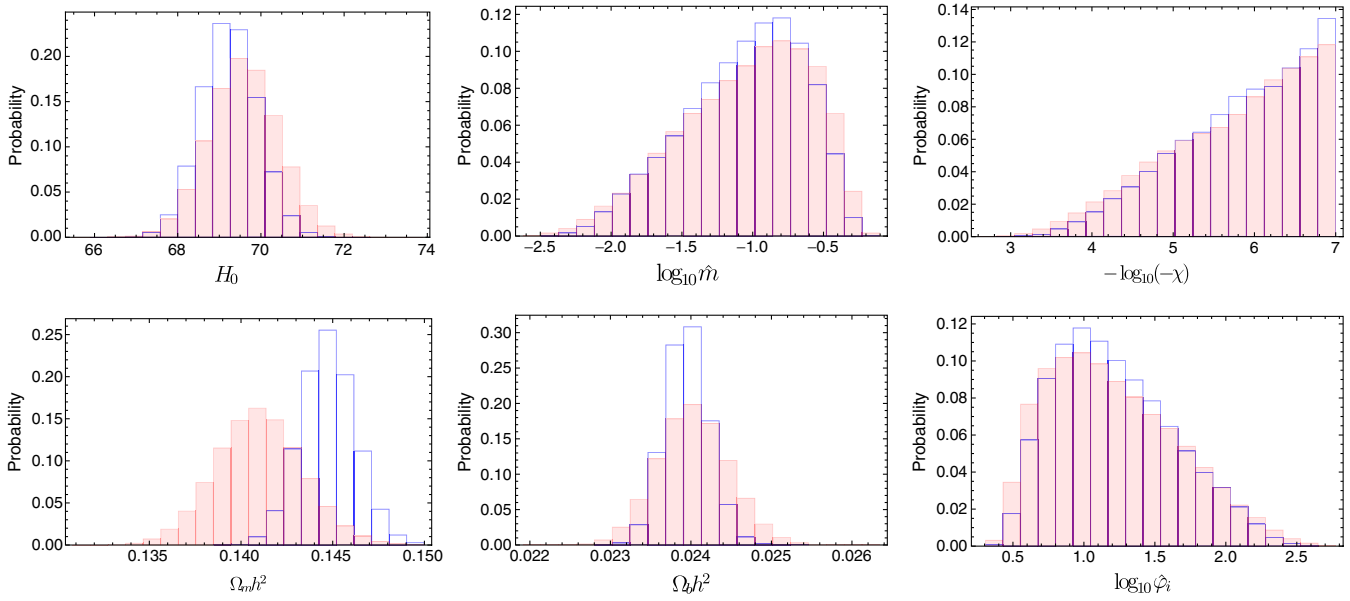

FIG. 3. Marginalized one-dimensional probability distributions of Hubble constant (H_0) and five model parameters [$\log_{10}\hat{m}$, $-\log_{10}(-\chi)$, $\Omega_m h^2$, $\Omega_b h^2$, $\log_{10}\hat{\varphi}_i$], favored by the current observations: $H(z)+\mathrm{SN}+\mathrm{BAO}+\mathrm{PLANCK}$ (blue) and $H(z)+\mathrm{SN}+\mathrm{BAO}+\mathrm{WMAP9}$ (red histograms), respectively.

calculation, we use $\log_{10}\hat{m}$, $-\log_{10}(-\chi)$, $\Omega_m h^2$, $\Omega_b h^2$, and $\log_{10}\hat{\varphi}_i$ as free parameters. The results are shown in Table I for a summary of parameter constraints with mean and 1σ confidence limits and in Fig. 3 for marginalized one-dimensional likelihood distributions of individual parameters. We can see that the result obtained with Planck data gives tighter constraints on model parameters. The best-fit locations in the parameter space are

$$(\log_{10}\hat{m}, -\log_{10}(-\chi), \Omega_m h^2, \Omega_b h^2, \log_{10}\hat{\varphi}_i) = (-1.314, 6.964, 0.141, 0.024, 1.47), \quad (4.33)$$

with a minimum chi-square of $\chi^2_{\mathrm{min}} = 588.391$ for the $H(z)+\mathrm{SN}+\mathrm{BAO}+\mathrm{WMAP9}$, and

$$(\log_{10}\hat{m}, -\log_{10}(-\chi), \Omega_m h^2, \Omega_b h^2, \log_{10}\hat{\varphi}_i) = (-1.270, 6.908, 0.145, 0.024, 1.42), \quad (4.34)$$

with $\chi^2_{\mathrm{min}} = 590.804$ for $H(z)+\mathrm{SN}+\mathrm{BAO}+\mathrm{PLANCK}$. The behaviors of Hubble parameter and SN distance modulus as a function of redshift are shown in Fig. 4. In Fig. 5, we also present the marginalized likelihood distributions for $(H_0, \log_{10}\hat{m})$ and $(\log_{10}\hat{\varphi}_i, \log_{10}\hat{m})$, which shows that the value of Hubble constant does not depend on the variation of photon mass while the initial value of $\hat{\varphi}$ decreases as the photon mass increases.

To assess the goodness of fit of our massive photon model, in Table I we present the parameter constraints for

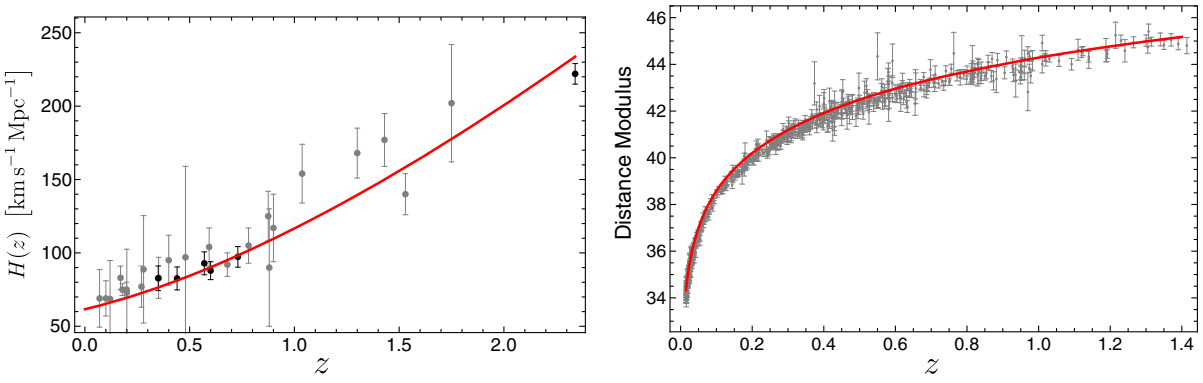

FIG. 4. (Left) Observed Hubble parameters versus redshift (grey and black dots with error bars; see text). (Right) The Hubble diagram for Union 2.1 compilation of SN type Ia. In both figures, the red curve represents the best-fit prediction of our model constrained with $H(z)$, SN, BAO, and CMB data sets.

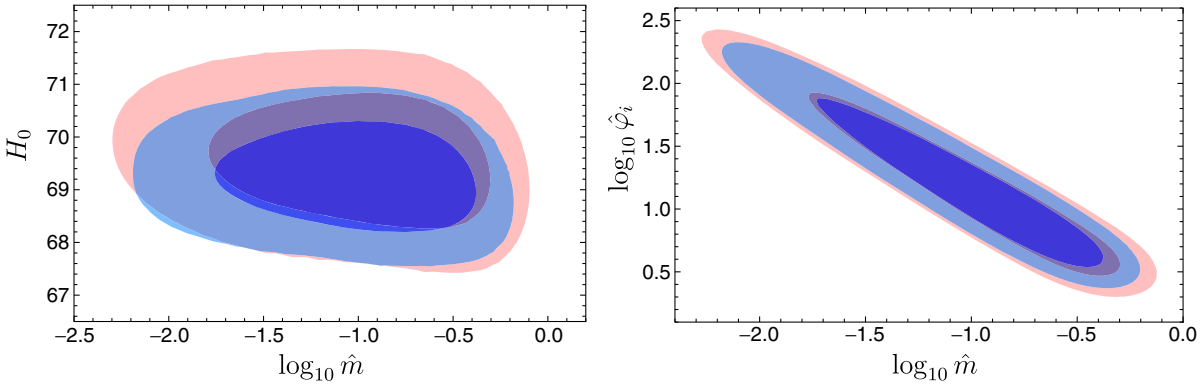

FIG. 5. Marginalized likelihood distributions for $(H_0, \log_{10}\hat{m})$ (left) and $(\log_{10}\hat{\varphi}_i, \log_{10}\hat{m})$ (right) with 68.3% and 95.4% confidence limits, obtained by the joint parameter estimation with $H(z) + \mathrm{SN} + \mathrm{BAO} + \mathrm{PLANCK}$ (blue) and $H(z) + \mathrm{SN} + \mathrm{BAO} + \mathrm{WMAP9}$ (red) data sets, respectively.

the ΛCDM model and list the value of the minimum reduced chi-square (χ^2_ν) for each case. The minimum reduced chi-square is defined as $\chi^2_\nu = \chi^2_{\mathrm{min}}/\nu$, where $\nu = N - n - 1$ is the number of degrees of freedom and N and n are the numbers of data points and free model parameters, respectively. In our analysis, $N = 618$, and $n = 5$ for our massive photon model and $n = 3$ for the ΛCDM model. Although the simple ΛCDM model gives a slightly better fit to the observational data with the smaller values of χ^2_{min} and χ^2_ν, we judge that our massive photon model fits the data reasonably well in the sense that the reduced chi-square is very close to unity.

We note that for our model to be compatible with observations the photon should have nonzero mass with $\log_{10}\hat{m} \approx -1$, which corresponds to the photon mass $m \approx 10^{-34}$ eV. Such a value is consistent with current experimental upper bound on the photon mass $m \leq 10^{-15}$ eV from the measurements of Earth's magnetic field [39], Pioneer-10 data of the Jupiter magnetic field [40], and $m \leq 10^{-27}$ eV from the Galactic magnetic fields [41].

V. CONCLUSION

In this paper, we investigated the cosmological implications of the massive Stueckelberg QED nonminimally coupled to the Einstein gravity, paying special attention to the possible role of the massive photon in relation to dark energy. We found that the theory allows a long period of current accelerating phase that closely mimics ΛCDM in which the acceleration of Universe is due to the nonvanishing photon mass governed by the relation $\Lambda \sim m^2$. A detailed numerical analysis in comparison with various data predicts the nonvanishing photon mass being on the order of $\sim 10^{-34}$ eV, which is consistent with the other upper limits available so far.

The cosmological evolution of the nonminimal SVT gravity theory exhibits a couple of interesting properties. The left panel of Fig. 2 shows that the dark-energy density of (2.18) has the same scaling behavior with the radiation energy density in the radiation-dominated epoch. In addition, during the intermediate state between the radiation and the constant dark-energy epoch, the behavior of dark-energy density mimics the pressureless matter; this can be seen clearly from the equation-of-state graph of Fig. 2. Then, this constant dark-energy-dominant era lasts for a long period of time (Fig. 2), in which the current acceleration of Universe takes place. During this period, the dark-energy density is practically given by an intriguing relation $\rho^{(\mathrm{de})} \sim m^2 M_p^2$.

We note that the scalar field stays almost constant (Fig. 1) before a relaxation to its natural value of zero begins to occur during the matter-dominated epoch. The analysis in Sec. III C shows that the Stueckelberg scalar field will ultimately relax to zero after going through a period of oscillations. Both the energy density and pressure decay as $1/a^3$ during the oscillations, but the pressure (and the temporal component) also oscillates in harmony with the scalar fields. Therefore, the analysis predicts a gradual deviation from ΛCDM in the future, and that the Universe will see the return of the matter-dominated epoch (not the pressureless dust, but the remnants of the scalar-temporal field component oscillations).

We also compared the massive photon model with the observational data of SN type Ia, Hubble parameter, BAO, and CMB measurements. According to MCMC methods, we obtained the best-fit values of the parameters (shown in Table I) by fixing the value of $\hat{\eta}$ to 0.9 and $\hat{\omega}$ to −0.35. It may be important to mention here that these fixed values of parameters $\hat{\eta}$ and $\hat{\omega}$ correspond to the decay mode during the matter-dominated epoch. Presumably, different values will not alter the numerical results much as long as these parameters are chosen to satisfy the decay condition (3.16), $\beta < 3$. We found that $m \sim 10^{-34}$ eV is allowed by the $H(z) + \mathrm{SN} + \mathrm{BAO} + \mathrm{CMB}$ data set for the massive Stueckelberg QED nonminimally coupled to the Einstein gravity. This is consistent with the most stringent upper

bounds on the photon mass listed by the Particle Data Group [14]. In addition, this result can give a highly precise estimation for the mass of the photon. We also found that the ΛCDM model is still compatible with our massive photon model.

We conclude with a final comment on $\rho^{(\mathrm{de})}|_0 \sim \Lambda M_p^2 \sim m^2 M_p^2$. It would be certainly impossible to perform any experiment to establish the exact vanishing of the photon mass, but the ultimate upper limit on the photon rest mass, m, can be estimated by using the uncertainty principle to be $m \approx \hbar/(\Delta t)c^2 \cong 10^{-34}$ eV for the current age of the universe. Our analysis with the observational data shows that this value is in agreement with the prediction of massive QED. It is also interesting to note that the relation $\Lambda \sim m^2$ provides a vacuum energy density $\Lambda_c^4 \sim \Lambda M_{\mathrm{p}}^2$ with IR cutoff $L \sim m^{-1}$, in accordance with the holographic constraint [7].

ACKNOWLEDGMENTS

We would like to thank the anonymous referee for valuable comments and C. Lee and W.-T. Kim for useful discussions. P. O. was supported by Basic Science Research Program through the National Research Foundation of Korea (NRF) funded by the Ministry of Education (Grant No. 2015R1D1A1A01056572). C. G. P. was supported by Basic Science Research Program through the National Research Foundation (NRF) of Korea funded by the Ministry of Science, ICT, and Future Planning (Grant No. 2013R1A1A1011107).

[1] A. G. Riess *et al.* (Supernova Search Team Collaboration), Observational evidence from supernovae for an accelerating universe and a cosmological constant, Astron. J. **116**, 1009 (1998).

[2] S. Perlmutter *et al.* (Supernova Cosmology Project Collaboration), Measurements of omega and lambda from 42 high redshift supernovae, Astrophys. J. **517**, 565 (1999).

[3] E. Komatsu *et al.* (WMAP Collaboration), Five-year Wilkinson Microwave Anisotropy Probe (WMAP) observations: Cosmological interpretation, Astrophys. J. Suppl. Ser. **180**, 330 (2009).

[4] S. Weinberg, The cosmological constant problem, Rev. Mod. Phys. **61**, 1 (1989); S. M. Carroll, W. H. Press, and E. L. Turner, The cosmological constant, Annu. Rev. Astron. Astrophys. **30**, 499 (1992); V. Sahni and A. A. Starobinsky, The case for a positive cosmological lambda-term, Int. J. Mod. Phys. D **09**, 373 (2000); T. Padmanabhan, Cosmological constant: The weight of the vacuum, Phys. Rep. **380**, 235 (2003); Dark energy: The cosmological challenge of the millennium, Curr. Sci. **88**, 1057 (2005); P. J. E. Peebles and B. Ratra, The cosmological constant and dark energy, Rev. Mod. Phys. **75**, 559 (2003).

[5] B. Ratra and P. J. E. Peebles, Cosmological consequences of a rolling homogeneous scalar field, Phys. Rev. D **37**, 3406 (1988); C. Wetterich, Cosmology and the fate of dilatation symmetry, Nucl. Phys. **B302**, 668 (1988); P. G. Ferreira and M. Joyce, Cosmology with a primordial scaling field, Phys. Rev. D **58**, 023503 (1998); E. J. Copeland, A. R. Liddle, and D. Wands, Exponential potentials and cosmological scaling solutions, Phys. Rev. D **57**, 4686 (1998); R. R. Caldwell, R. Dave, and P. J. Steinhardt, Cosmological Imprint of an Energy Component with General Equation of State, Phys. Rev. Lett. **80**, 1582 (1998).

[6] S. A. Bludman, Tracking quintessence would require two cosmic coincidences, Phys. Rev. D **69**, 122002 (2004); J. Lee, T. H. Lee, P. Oh, and J. Overduin, Cosmological coincidence without fine tuning, Phys. Rev. D **90**, 123003 (2014).

[7] A. G. Cohen, D. B. Kaplan, and A. E. Nelson, Effective Field Theory, Black Holes, and the Cosmological Constant, Phys. Rev. Lett. **82**, 4971 (1999).

[8] N. Arkani-Hamed, L. J. Hall, C. F. Kolda, and H. Murayama, A New Perspective on Cosmic Coincidence Problems, Phys. Rev. Lett. **85**, 4434 (2000).

[9] L. C. Tu, J. Luo, and G. T. Gillies, The mass of the photon, Rep. Prog. Phys. **68**, 77 (2005); L. B. Okun, Photon: History, mass, charge, Acta Phys. Pol. B **37**, 565 (2006); A. S. Goldhaber and M. M. Nieto, Photon and graviton mass limits, Rev. Mod. Phys. **82**, 939 (2010).

[10] H. Ruegg and M. Ruiz-Altaba, The Stueckelberg field, Int. J. Mod. Phys. A **19**, 3265 (2004).

[11] M. Suzuki, Slightly massive photon, Phys. Rev. D **38**, 1544 (1988).

[12] J. Heeck, How Stable Is the Photon?, Phys. Rev. Lett. **111**, 021801 (2013).

[13] A. Accioly, J. Helayel-Neto, and E. Scatena, Combining general relativity, massive QED and very long baseline interferometry to gravitationally constrain the photon mass, Phys. Lett. A **374**, 3806 (2010).

[14] K. Hagiwara *et al.* (Particle Data Group Collaboration), Review of particle properties, Phys. Rev. D **66**, 010001 (2002).

[15] L. H. Ford, Inflation driven by a vector field, Phys. Rev. D **40**, 967 (1989); W. Zimdahl, D. J. Schwarz, A. B. Balakin, and D. Pavon, Cosmic anti-friction and accelerated expansion, Phys. Rev. D **64**, 063501 (2001); C. Armendariz-Picon, Could dark energy be vector-like?, J. Cosmol. Astropart. Phys. 07 (2004) 007; V. V. Kiselev, Vector field as a quintessence partner, Classical Quantum Gravity **21**, 3323 (2004); M. Novello, S. E. Perez Bergliaffa, and J. Salim, Nonlinear electrodynamics and the acceleration of the universe, Phys. Rev. D **69**, 127301 (2004);

C. G. Boehmer and T. Harko, Dark energy as a massive vector field, Eur. Phys. J. C **50**, 423 (2007); T. Koivisto and D. F. Mota, Vector field models of inflation and dark energy, J. Cosmol. Astropart. Phys. 08 (2008) 021.

[16] J. Beltran Jimenez and A. L. Maroto, A cosmic vector for dark energy, Phys. Rev. D **78**, 063005 (2008); Vector models for dark energy, arXiv:0807.2528; Cosmological electromagnetic fields and dark energy, J. Cosmol. Astropart. Phys. 03 (2009) 016.

[17] J. Kim, S. Kouwn, P. Oh, and C. G. Park, Dark aspects of massive spinor electrodynamics, J. Cosmol. Astropart. Phys. 07 (2014) 001.

[18] J. B. Jimenez, E. Dio, and R. Durrer, A longitudinal gauge degree of freedom and the Pais Uhlenbeck field, J. High Energy Phys. 04 (2013) 030; Ö. Akarsu, M. Arik, N. Katirci, and M. Kavuk, Accelerated expansion of the universe à la the Stueckelberg mechanism, J. Cosmol. Astropart. Phys. 07 (2014) 009.

[19] I. J. R. Aitchison, *An Informal Introduction to Gauge Field Theories* (Cambridge University Press, Cambridge, 1982).

[20] S. Deser, The limit of massive electrodynamics, Ann. Inst. Henri Poincaré **A16**, 79 (1972).

[21] R. W. Hellings and K. Nordtvedt, Vector-metric theory of gravity, Phys. Rev. D **7**, 3593 (1973).

[22] C. M. Will, *Theory and Experiment in Gravitational Physics* (Cambridge University Press, Cambridge, England, 1993), p. 129; J. Beltran Jimenez and A. L. Maroto, Viability of vector-tensor theories of gravity, J. Cosmol. Astropart. Phys. 02 (2009) 025.

[23] B. Bertotti, L. Iess, and P. Tortora, A test of general relativity using radio links with the Cassini spacecraft, Nature (London) **425**, 374 (2003).

[24] N. Metropolis, A. W. Rosenbluth, M. N. Rosenbluth, A. H. Teller, and E. Teller, Equation of state calculations by fast computing machines, J. Chem. Phys. **21**, 1087 (1953); W. K. Hastings, Monte Carlo sampling methods using Markov chains and their applications, Biometrika **57**, 97 (1970).

[25] A. Abrahamse, A. Albrecht, M. Barnard, and B. Bozek, Exploring parameter constraints on quintessential dark energy: The pseudo-Nambu-Goldstone-boson model, Phys. Rev. D **77**, 103503 (2008).

[26] C. Zhang, H. Zhang, S. Yuan, T. J. Zhang, and Y. C. Sun, Four new observational $H(z)$ data from luminous red galaxies in the Sloan Digital Sky Survey data release seven, Res. Astron. Astrophys. **14**, 1221 (2014); J. Simon, L. Verde, and R. Jimenez, Constraints on the redshift dependence of the dark energy potential, Phys. Rev. D **71**, 123001 (2005); M. Moresco *et al.*, Improved constraints on the expansion rate of the Universe up to $z \sim 1.1$ from the spectroscopic evolution of cosmic chronometers, J. Cosmol. Astropart. Phys. 08 (2012) 006; D. Stern, R. Jimenez, L. Verde, M. Kamionkowski, and S. A. Stanford, Cosmic chronometers: Constraining the equation of state of dark energy. I: H(z) Measurements, J. Cosmol. Astropart. Phys. 02 (2010) 008.

[27] C. H. Chuang and Y. Wang, Modeling the anisotropic two-point galaxy correlation function on small scales and improved measurements of $H(z)$, $D_A(z)$, and $\beta(z)$ from the Sloan Digital Sky Survey DR7 luminous red galaxies, Mon. Not. R. Astron. Soc. **435**, 255 (2013); C. Blake *et al.*, The WiggleZ Dark Energy Survey: Joint measurements of the expansion and growth history at $z < 1$, Mon. Not. R. Astron. Soc. **425**, 405 (2012); L. Samushia *et al.*, The clustering of galaxies in the SDSS-III DR9 Baryon Oscillation Spectroscopic Survey: Testing deviations from Λ and general relativity using anisotropic clustering of galaxies, Mon. Not. R. Astron. Soc. **429**, 1514 (2013); T. Delubac *et al.* (BOSS Collaboration), Baryon acoustic oscillations in the Ly forest of BOSS DR11 quasars, Astron. Astrophys. **574**, A59 (2015); X. Ding, M. Biesiada, S. Cao, Z. Li, and Z. H. Zhu, Is there evidence for dark energy evolution? Astrophys. J. **803**, L22 (2015).

[28] N. Suzuki *et al.*, The Hubble Space Telescope Cluster Supernova Survey: V. Improving the dark energy constraints above $z > 1$ and building an early-type-hosted supernova sample, Astrophys. J. **746**, 85 (2012).

[29] M. Goliath, R. Amanullah, P. Astier, A. Goobar, and R. Pain, Supernovae and the nature of the dark energy, Astron. Astrophys. **380**, 6 (2001); S. Nesseris and L. Perivolaropoulos, Comparison of the legacy and gold type Ia supernovae dataset constraints on dark energy models, Phys. Rev. D **72**, 123519 (2005).

[30] D. J. Eisenstein *et al.* (SDSS Collaboration), Detection of the baryon acoustic peak in the large-scale correlation function of SDSS luminous red galaxies, Astrophys. J. **633**, 560 (2005).

[31] D. J. Eisenstein and W. Hu, Baryonic features in the matter transfer function, Astrophys. J. **496**, 605 (1998).

[32] F. Beutler, C. Blake, M. Colless, D. H. Jones, L. Staveley-Smith, L. Campbell, Q. Parker, W. Saunders, and Fred Watson, The 6dF Galaxy Survey: Baryon acoustic oscillations and the local Hubble constant, Mon. Not. R. Astron. Soc. **416**, 3017 (2011).

[33] N. Padmanabhan, X. Xu, D. J. Eisenstein, R. Scalzo, A. J. Cuesta, K. T. Mehta, and E. Kazin, A 2 percent distance to $z = 0.35$ by reconstructing baryon acoustic oscillations—I. Methods and application to the Sloan Digital Sky Survey, Mon. Not. R. Astron. Soc. **427**, 2132 (2012); L. Anderson, E. Aubourg, S. Bailey, D. Bizyaev, M. Blanton, A. S. Bolton, J. Brinkmann, J. R. Brownstein *et al.*, The clustering of galaxies in the SDSS-III Baryon Oscillation Spectroscopic Survey: Baryon acoustic sscillations in the data release 9 spectroscopic galaxy sample, Mon. Not. R. Astron. Soc. **427**, 3435 (2012).

[34] C. Blake, S. Brough, M. Colless, C. Contreras, W. Couch, S. Croom, D. Croton, T. Davis *et al.*, The WiggleZ Dark Energy Survey: Joint measurements of the expansion and growth history at $z < 1$, Mon. Not. R. Astron. Soc. **425**, 405 (2012).

[35] G. Hinshaw *et al.* (WMAP Collaboration), Nine-year Wilkinson Microwave Anisotropy Probe (WMAP) observations: Cosmological parameter results, Astrophys. J. Suppl. Ser. **208**, 19 (2013).

[36] P. A. R. Ade *et al.* (Planck Collaboration), Planck 2013 results. XVI. Cosmological parameters, Astron. Astrophys. **571**, A16 (2014).

[37] W. Hu and N. Sugiyama, Small scale cosmological perturbations: An analytic approach, Astrophys. J. **471**, 542 (1996).
[38] D. L. Shafer and D. Huterer, Chasing the phantom: A closer look at type Ia supernovae and the dark energy equation of state, Phys. Rev. D **89**, 063510 (2014).
[39] E. Fischbach, H. Kloor, R. A. Langel, A. T. Y. Liu, and M. Peredo, New Geomagnetic Limits on the Photon Mass and on Long-Range Forces Coexisting With Electromagnetism, Phys. Rev. Lett. **73**, 514 (1994).
[40] L. Davis, Jr., A. S. Goldhaber, and M. M. Nieto, Limit on the Photon Mass Deduced from Pioneer-10 Observations of Jupiter's Magnetic Field, Phys. Rev. Lett. **35**, 1402 (1975).
[41] R. Lakes, Experimental Limits on the Photon Mass and Cosmic Magnetic Vector Potential, Phys. Rev. Lett. **80**, 1826 (1998); G. V. Chibisov, Astrophysical upper limits on the photon rest mass, Usp. Fiz. Nauk **119**, 551 (1976) [Sov. Phys. Usp. **19**, 624 (1976)].